IJVS 2017; 12(2); Serial No:27

IRANIAN JOURNAL OF VETERINARY SURGERY (IJVS)
WWW.IVSA.IR

Original Article

The healing effect of chitosan supported nano-CeO2 on experimental excisional wound infected with *pseudomonas aeruginosa* in rat

Ako Shabrandi[1], Saeed Azizi*[1], Rahim Hobbenaghi[2], Abdolghafar Ownagh[3], Sajjad Keshipour[4]

Abstract

Objective- The healing effect of chitosan supported cerium oxide nanoparticles (nano-CeO2) on cutaneous experimental excisional wound infected with *pseudomonas aeruginosa* was studied in rat.

Design- Experimental Study.

Animals- Sixty male albino rats.

Procedures- The chitosan supported nano-CeO2 hydrogel was prepared and characterized using Fourier-transform infrared spectroscopy (FT-IR), Energy Dispersive X-ray Spectroscopy (EDX), X-ray powder diffraction (XRD), Scanning Electron Microscopy (SEM) and Transmission Electron Microscopy (TEM). The wound was infected with *p. aeruginosa* and in positive control (PC) group it was treated with silver sulfadiazine ointment with no treatment in negative control (NC) group. The infected wound was treated with chitosan suspension-gel, cerium oxide nanoparticles solution or chitosan supported-CeO2 nanoparticle gel in the treatment groups. The rats were randomized into five groups (n=12). Each group was subdivided into three subgroups of four animals each and studied 3, 7 and 14 days post-wounding.

Results- Plantimetry, histopathological assessments and hydroxyprolin content showed better and faster healing of the wounds in the treatment groups, particularly in chitosan supported-CeO2 nanoparticle gel (ChCe) group compared to the NC group ($P< 0.05$). Using by Ferric Reducing Antioxidant Power (FRAP) the total antioxidant capacity was statistically higher in treatment groups compared to NC group ($p< 0.05$). The bacterial numbers were significantly lower in ChCe and cerium oxide nanoparticles solution (Ce) groups compared to chitosan (CH) group on day 3 post-wounding ($P< 0.05$).

Conclusion and Clinical Relevance-Topical application of the chitosan supported nano-CeO2 particles on the infected wound enhanced tissue total antioxidant capacity, reduced the bacterial count, accelerated proliferation and migration of fibroblasts and keratinocytes, increased hydroxyproline level and neovascularization scale of the healing wound. Chitosan supported nano-CeO2 hydrogel could be suggested as an alternative therapy for treating of the infected wound.

Key word: nano-CeO2, chitosan, *pseudomonas aeruginosa*, wound healing, rat.

Received: 6 August 2017; **Accepted:** 22 November 2018; **Online:** 19 Fbreuary 2018

Introduction

Wound healing is a well-scored and complex physiological dynamic process which is triggered by tissue injury and ends by regeneration or repair.[1,2] Proliferation and migration of fibroblasts and keratinocytes, also the growth of vascular endothelial cells to form new blood vessels are essential for wound Healing.[3] Clean wounds usually heal without delay and undesired medical complications. Impairment of wound healing by infection can cause significant pain and discomfort for the patient. Early recognition with early appropriate and effective intervention is critical in treatment of the infected wounds.[4]

Pseudomonas species is one of the primarily opportunistic pathogen responsible for infection of the wounds in hospitalized patients, patients with inherent immunity defects or after trauma.[2] These organisms also possess many structural factors, enzymes, and toxins that enhance their virulence and render them resistant to the most commonly used antibiotics.[2] *P.*

[1]Department of Surgery and Diagnostic Imaging, [2]Department of Pathobiology, Faculty of Veterinary Medicine, Urmia University, Urmia, Iran
[3]Department of Microbiology, Faculty of Veterinary Medicine, Urmia University, Urmia, Iran
[4]Department of Nanochemistry, Nanotechnology Research Centre, Urmia University, Urmia, Iran
***Corresponding address: Address all correspondence to Saeed Azizi, (DVM, DVSc). E-Mail: s.azizi@urmia.ac.ir**

DOI: 10.22034/ivsa.2017.94632.1122

aeruginosa is inherently resistant to many antibiotics and can mutate to even more resistant strains during therapy.[5] Nowadays, silver sulphadiazine as an effective and painless topical ointment is used to control *P. aeruginosa* and other infections in burn wounds.[6,7]

Sustained oxidative stress contributes to impair wound healing process that results in non-healing wounds.[8] Cells within and surrounding wounds experience elevated levels of reactive oxygen and nitrogen species and levels of natural endogenous antioxidants that are diminished in impaired wounds.[9] Exogenous antioxidants individually or in combination with nanoparticle have been reported to enhance wound healing.[10-15]

Cerium oxide nanoparticles (CeO2-NPs), a therapeutic agent to treat a number of diseases, bear minimal toxicity to tissues and help protect tissue from various forms of reactive oxygen species (ROS).[16] CeO2-NPs have also been used to enhance wound healing *in vitro* and *in vivo*.[17] Chitosan is a biodegradable polysaccharide, with hemostatic, bacteriostatic and wound healing properties and has been used in a wide range of biomedical applications.[18,19] The mechanisms of antimicrobial activity of chitosan have been reported by others.[20-23]

Wound infection continues to be a challenging problem in practice and an overall delay in the healing process of the infected wounds are usually encountered and topical antibiotics have limited success to control the infection.[5] The rise of antimicrobial resistance has been encouraging for investigators to study other antimicrobials like nanoparticles that are not tolerated by bacteria. The antibacterial effect of Ceo2-NP on *Staphylococcus aureus* and *Streptococcus mutans* has already been reported.[22-26] The purpose of the present study was to investigate the healing effects of chitosan supported nano-CeO2 on cutaneous experimental excisional wound infected with *P. aeruginosa* in a rat model.

Materials and Methods

All reagents were research grade and purchased from Sigma-aldrich and used without further purification. Chitosan was purchased from Sigma-aldrich with 2000 molecular weight (99.98% Purity). Scanning Electron Microscopy (SEM) and EDS was performed with SEM of TSCAN company. Transmission Electron Microscopy (TEM) was performed by LEO912AB electron microscope at 200 KeV. X-ray powder diffraction (XRD) data were collected on an XD-3A diffractometer using Cu K_α radiation. Ce determination was carried out on an FAAS (Shimadzu model AA-680 atomic absorption spectrometer), using an air-acetylene flame with molybdenum hollow cathode lamp at 313 nm.

Low molecular Chitosan powder (0.5 g) (deacetylation degree of 75–85%) was dispersed in 50 mL of 1.0% w/w of glacial acetic acid (Aldrich) and sonicated vigorously two hours to achieve dissolution. A solution of PP was prepared by dissolving in water at 500 mg/mL, followed by keeping at 4 °C until a homogenous solution was formed. Different amounts of polyphosphate were aliquoted into the chitosan solution to achieve a 2.5% w/w ratio in chitosan.

Preparation of chitosan supported nano-CeO_2

Chitosan (0.5 g, MW=2000) was dissolved in 25 mL acetic acid (1% v/v) under vigorous stirring. The resulted solution after sonication for 1 h gave a bubble free gel. $Ce(NO_3)_3$ (1.3305 g) was added to the obtained gel under stirring, and stirring continued for 48 h. The pH of the mixture was adjusted in 3 with addition of concentrate HCl. The mixture was treated with H2O2 (313 μL, 12%) for oxidation of Ce(III) to nano-CeO2. After 3 days, 40 mL acetone was added to the reaction vessel and the mixture was filtered off to give nano-CeO_2 as a yellow powder after drying in oven (50 °C).

Animals

Sixty male albino rats weighing 250-300 g, 3–4 month-old were used in this study. They were brought to our central animal facility and caged individually for a 2-week acclimatization period and were maintained at constant temperature (23 ± 1°C) and 70% humidity on a 12:12-h light-dark cycle. They were maintained on rat standard pellet diet and corn, and provided with water *ad-libitum* throughout the experiment. The procedures were performed based on the guidelines of the Ethics Committee of the International Association for the Study of pain.[27] The University Research Council approved all experiments.

Rats were divided into five groups (n= 12), randomly: In negative control the wound was infected by topical application of *p. aeruginosa* (10^8 CFU/mL) solution with no further treatment (NC). In positive control, the infected wound was treated by topical application of 1% silver sulfadiazine ointment (PC). In CH group, the infected

wound was treated by topical application of chitosan suspension (30 µl of 1% chitosan gel). In Ce group the infected wound was treated by topical application of 20 µL of a 10 µM solution of cerium oxide nanoparticles and in ChCe group, the infected wound was treated by topical application of 30 µL of a 3.7 w/w% gel chitosan supported-CeO2nanoparticle. Each group was subdivided into three subgroups of four animals each and studied 3, 7 and 14 days post-wounding.

An excision wound model was used to study wound healing process. Rats were anesthetized using intra peritoneal injection of ketamine 60 mg/kg and xylazine 5mg/kg (alfasan holand). The back of rats was shaved using razor blade and the hair was carefully removed from the back of the animals. The rats were placed on a paper towel and their back was wiped with a sufficient amount of 70 % alcohol. Two folds of rat dorsum skin equidistant from midline of the back were made by lifting them and a 10 mm dermal biopsy was taken with homemade sterile punch. Technically, this resulted in two symmetrical full thickness of 10 mm diameter excision circle wounds extending through the panniculus carnosus about 10–15 mm distance from each other without any underlying tissue damage. To avoid motion artifacts during planimetry measurements the wounds were made just above the bridge of the back. Donut-shaped 0.5mm-thick silicone splints with a diameter of two times than of the wound area was made and centered and then fixed to the skin with both immediate bonding adhesive and 4-0 nylon interrupted sutures. The rats were placed in their individual cages warmed by a heater and allowed to recover fully from anesthesia.

Bacterial strain and culture conditions

To infect wounds, A clinical nosocomial gram negative *p. aeruginosa* (PTCC1310) purchased from Persian Type Culture Collection was used. In brief, the strain was grown on nutrient agar. After 24 h, bacterial cultures were harvested, and a bacterial suspension was prepared and compared to a McFarland standard. For the infected wounds, bacterial suspension containing approximately 10^8 CFU/mL of *P. aeruginosa* was applied by a 50 µL pipette tip into the wound bed once immediately after wounding (Inocula of McFarland standards phase OD at 600nm=0.6–0.8; 10^8 cells/mL).Wound treatment was done 30 minutes after inoculation of the bacteria and the wound treatments were done once daily for seven consecutive days. To avoid further intervention the wounds were not dressed in the experimental animals.

Planimetry

To follow the wound healing process, changes in wound area were measured regularly by digital photograph on the day of surgery and on days 3, 7, 14 after surgery and the rate of wound closure was calculated using the following formula:

Percent wound contraction = wound area /primary wound area × 100).[28]

Wound area was calculated as a percent area of the original wound. . The wound area was calculated using Photo Shop CS6 software.

There was no mortality during the study period. The rats were euthanized under general anesthesia on days 3, 7 and 14 post-wounding for histological, microbiological, hydroxyproline and FRAP studies.

Histological examination

In each subgroup 3 wounds were selected. The obtained biopsy specimens included the central part of the wounds. The specimens were fixated in 10 percent buffered formalin, dehydrated through a graded ethanol concentration series, cleared in xylene, and embedded in paraffin wax. The samples underwent routine histological processing with hematoxylin and eosin (H & E) and Masson's trichrome (MT) stains. Semi-quantitative method was used to evaluate re-epithelialization, inflammatory cell infiltration, fibroblast proliferation, neovascularization and collagen deposition. Sections were evaluated according to the scale: 0, 1, 2, 3, 4 by two independent observers.[29] The number of cells was counted in one high resolution field of each section.[30]

Hydroxyproline assessment

Hydroxyproline content, used as an index for the presence of collagen, was determined in wounds using a standard biochemical assay. In each subgroup, two rats were selected for hydroxyproline content of single individual wounds.[31] Briefly, the frozen tissue was hydrolyzed in 2 ml of 6 NHCl overnight at 110°C. The reaction was neutralized with 2.5 NNaOH and diluted 40-fold with distilled water. One ml of a 0.05M chloramine T solution was added to 2 ml of the neutralized/diluted

solution and incubated for 20 min at room temperature. One mL of 3.15 M perchloric acid was added, and the solution was incubated for 5 min at room temperature. One mL of 20% p-dimethylaminobenzaldehyde was subsequently added, and the mixture was incubated for 20 min at room temperature. The samples were then cooled with cold tap water. The hydroxyproline level (µg/mg) was determined spectrophotometrically at 557 nm.

FRAP assessment

The Ferric Reducing Antioxidant Power (FRAP) assay is based on the reduction of ferric ions to ferrous ions by the effect of the reducing power of the plasma (or tissue) constituents. The antioxidative activity is estimated by measuring the increase in absorbance caused by the formation of ferrous ions from FRAP reagent containing TPTZ (2,4,6-tripyridyl-s-triazine) and $FeCl_2$.6H2O. Three mL of freshly prepared and warm (37 °C) FRAP reagent 1 mL (10 mM) of 2,4,6 tripyridyl-s-triazine (TPTZ) solution in 40 mMHCl, 1 mL 20 mM FeCl2.6 H2O, 10 mL of 0.3 M acetate buffer (pH 3.6) was mixed with 0.375 mL distilled water and 0.025 mL of test samples. The absorbance of developed color in organic layer was measured spectrophotometrically at 593 nm and data were presented by scale µmol/ml. The readings at 180 s were selected for calculation of FRAP values.[32]

Quantitative microbiological analysis

To quantify bacterial colonization, two rats in each subgroup were selected and wounds were collected. The standard plate count method was used to count the bacteria per gram of tissue sample. Breifly, samples were diluted, plated in triplicate, and incubated over night at 37 °C for 24 hours. Following incubation, the enumeration of viable bacteria was performed. The outcome measure of efficacy of nanoparticle treatment was the mean number of bacteria in the treated wounds (log_{10} CFU/wound) compared to that of the control wounds.[33]

Statistical analysis

Data calculations for all parameters were performed using IBM SPSS Statistics 23 software. Wound closure in groups was assessed by planimetry and data were presented as a mean ± standard error. For each histological parameter mean values ± SEM were calculated. Multiple comparison tests were used to compare the polymorphonuclear (PMNL) cells ratios, percentage of re-epithelization and other histological assessments. For microbiological analysis the data were compared using a logarithmic scale owing to the wide variations in number of colony-forming units between cultures and values were reported as means ± SE. One-way ANOVA followed by Tukey statistical test was done to analyze planimetry, hydroxyproline content, FRAP assessment and microbiological analyses. The effect of time was analyzed using an ANOVA on repeated measure.[34] Statistical significance was set at $p < 0.05$

Results

Characterization of chitosan supported nano-CeO2

Chitosan supported nano-CeO2 was characterized with Fourier-transform infrared spectroscopy (FT-IR), Energy Dispersive X-ray Spectroscopy (EDX), Flame Atomic Absorption Spectroscopy (FAAS), SEM and TEM. The FT-IR spectrum of Nano-composite showed a new absorption band at 1534 cm^{-1} compared to chitosan spectrum (Fig 1). The new absorption band of chitosan supported nano-CeO_2 was attributed to the CeO_2.[31]

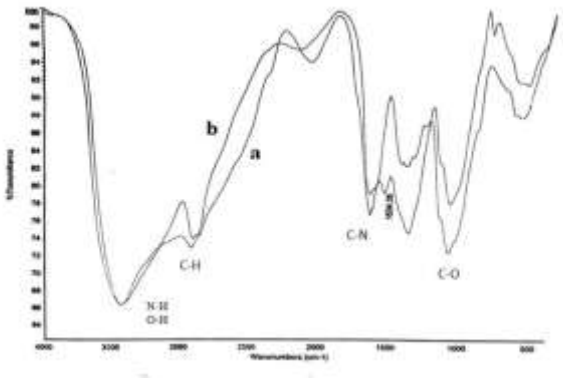

Figure 1. The Fourier-transform infrared spectroscopy (FT-IR) spectra of chitosan (a) and chitosan supported nano-CeO_2 (b)

EDX analysis is a common method for approving the existence of elements on the nano-composites. The EDX analysis of chitosan supported nano-CeO_2 showed that Ce was successfully loaded on the nano-composite (Fig 2). Cerium loading on the nano-composite was obtained 37 w/w% using FAAS analysis.

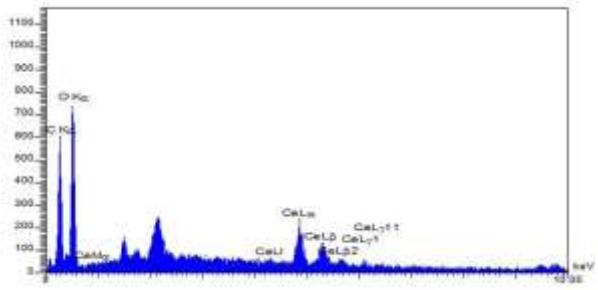

Figure 2. The Energy Dispersive X-ray Spectroscopy (EDX) analysis of chitosan supported nano-CeO_2

The XRD pattern of chitosan supported nano-CeO2 showed characteristic peaks of chitosan at 2θ= 24° and 40°. New characteristic peaks of nano-CeO2 particles were observed in the XRD pattern of nano-composite (Fig 3). Diffraction peaks of nano-CeO2 (111), (200), (220) and (400) were observable in the XRD pattern.

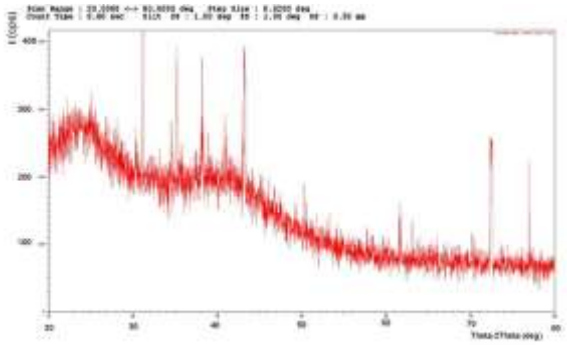

Figure 3. The X-ray powder diffraction (XRD) pattern of chitosan supported CeO2

TEM micrograms of the nano-composite were prepared to investigate the size and shapes of CeO_2 nanoparticles (Fig 4). A homogeneous distribution of CeO_2 nanoparticles was obtained on the chitosan surface. TEM micrograms approved the presented approach as a convenient route for the synthesis of chitosan supported nano-CeO_2 with homogeneous distribution of nano-CeO_2 on the support. Particle size for the nanoparticles was determined with maximum size distribution range of 4.9-6.2 nm. There were not any CeO2 nanoparticles on the chitosan supported nano-CeO_2 in SEM micrograph due to their fine structure. However, the morphology of the chitosan was observed (Fig 5).

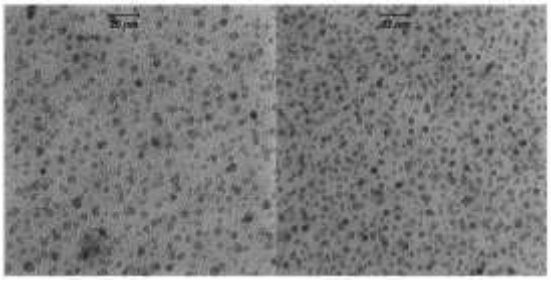

Figure 4. The Transmission Electron Microscopy (TEM) micrograms of chitosan supported CeO_2

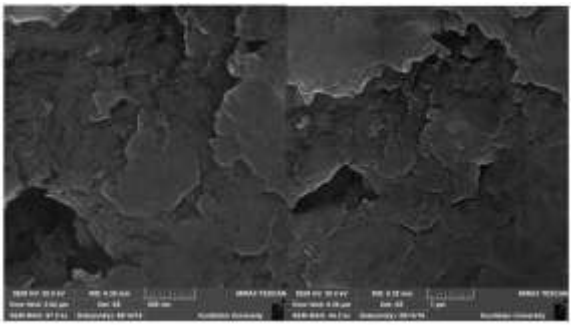

Figure 5. The Scanning Electron Microscope (SEM) analysis of chitosan supported nano-CeO_2

Planimetry

The results of the wound healing process among different groups are shown in figures 6 and 7. There was a statistically significant difference in wound area between negative control group and treatment groups throughout the study period ($P < 0.05$). The rate of wound closure was higher in ChCe group compared to CH and Ce groups, however, these differences were not statistically significant ($P>0.05$).

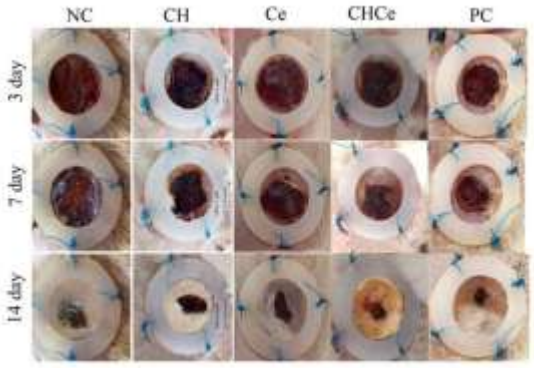

Figure 6. Serial photographs of wounds on different days in experimental groups.NC: Infected and not treated, CH: Infected and treated by chitosan, Ce: Infected and treated by cerium oxide nanoparticles, ChCe: Infected and treated by chitosan supported cerium nano particle, PC: Infected and treated by 1% silver sulphadiazin ointment.

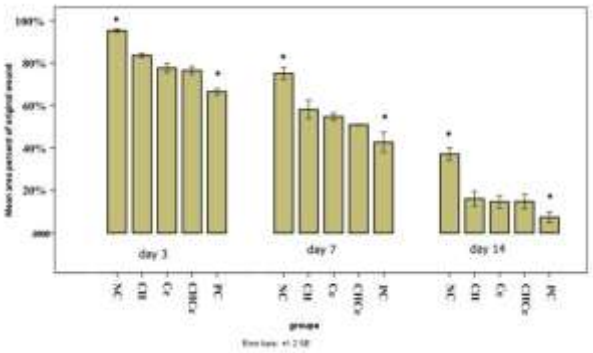

Figure 7. The mean percent of area reduction among different groups in the study period.

Histological assessment

Re-epithelialization was determined measuring the original width of the wound and measuring the re-epithelialized portions of the wound .There was a significant difference between NC group and treatment groups throughout study period ($P< 0.05$). The re-epithelialization percent in group ChCe (50% and 92% on days 7 and 14, respectively) was significantly different from those of NC group (30% and 60% on days 7 and 14, respectively. Better re-epithelialization was achieved in PC group, however, there was not significant difference in re-epithelialization percent between PC group and other treatment groups ($P>0.05$).

Infiltration of the PMNL cells was significantly lower in the treatment groups compared to NC group throughout the study period ($P < 0.05$). Infiltration of the PMNL cells scale was 3, 2 and 1 for PC group on days 3, 7 and 14, respectively. Infiltration of the PMNL cells scale was 2 for ChCe group on day 3 which was comparable to PC group. There was no significant difference in PMNL cells infiltration in the treatment groups compared to PC group ($P>0.05$).

The fibroblast scales were 1 and 2 in the treatment groups which were significantly higher than those of NC group which were 0 and 1 on days 3 and 7, respectively ($P< 0.05$). Otherwise, the fibroblast scale was significantly higher in NC group (scale 3) compared to the treatment groups (scale 2) on day 14 ($P< 0.05$).

Collagen content scale was significantly higher in the treatment groups compared to NC group in the study period ($P< 0.05$). The collagen content scale in ChCe group was comparable to those of PC group in the study period (Scale 1, 3 and 4 on days 3, 7 and 14, respectively) (Fig 8).

The neovascularization scale in the treatment groups (scale 4) was significantly higher than those of NC group (scale 2) on day 7 ($P < 0.05$). There was not significant differences in neovascularization scale between NC group (scale 3) compared to the treatment groups (scale 3) on day 14 ($P>0.05$).

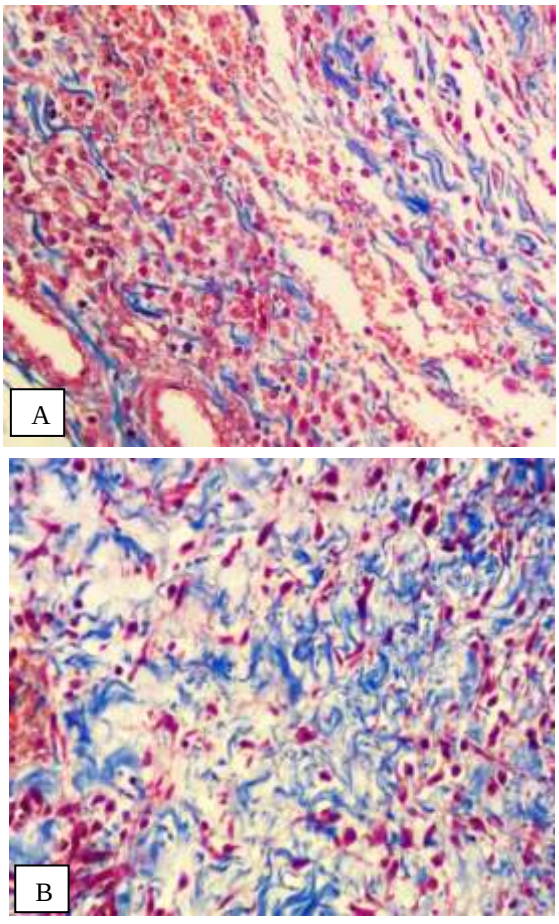

Figure 8. Histological micrograph of (A) NC group on day 7 after wounding and (B) CHce group on day 7 after wounding (Masson's trichrome staining, ×40).

Hydroxyproline assessment

Levels of hydroxyproline in different groups are in Figure 9. There was significant difference in Hydroxyproline content between the treatment groups and NC group in the study period (P < 0.05). Levels of hydroxyproline in the treatment groups were comparable to PC group.

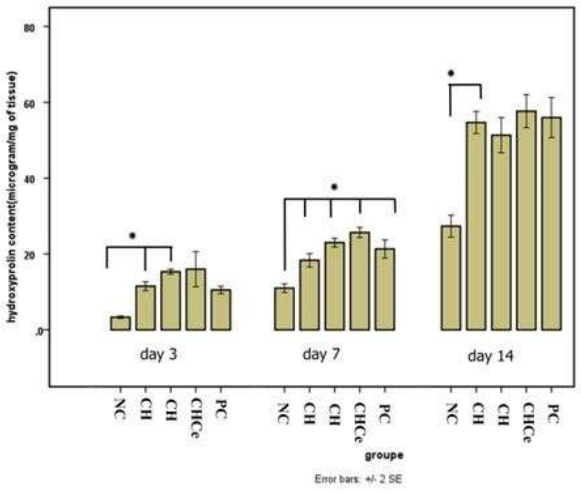

Figure 9: the hydroxyproline value in wounds.

Total antioxidant capacity (TAC)

The total antioxidant capacity in different groups is shown in Figure 10. The total antioxidant capacity was statistically significant in treatment groups compared to NC group in the study period (P < 0.05). The total antioxidant capacity in the treatment groups was comparable to the PC group on days 3 and 7 post-wounding. The total antioxidant capacity was statistically significant in ChCe group compared to those of CH group, Ce group and PC group, only on day 14 (P< 0.05).

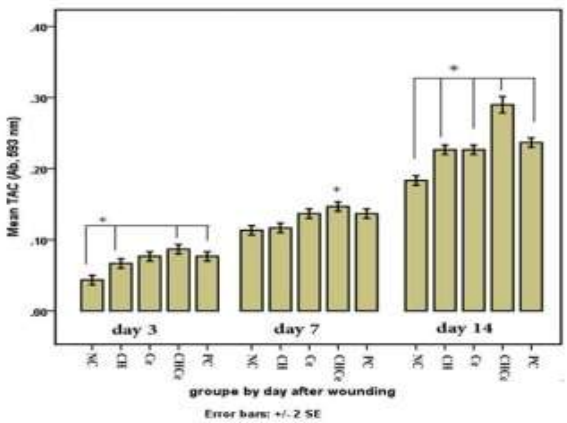

Figure 10. The total antioxidant capacity in experimental groups.

Microbiological analysis

Figure 11 shows the mean number of bacteria $\log_{10}$ CFU/wound in different groups. The mean bacterial counts from NC group were 8.8±0.3 $\log_{10,}$ 9.21±0.24 $\log_{10}$and 7.06±0.19 $\log_{10}$CFU/wound on days 3, 7 and 14 post-infection, respectively. The bacterial counts were significantly lower in ChCe (6.65±0.09 $\log_{10}$) and Ce (6.63±0.03 $\log_{10}$) groups compared to CH (7.86±0.26 $\log_{10}$), group on day 3 post-wounding (P < 0.05). The mean number of the bacteria per gram of tissue in CH, Ce and ChCe groups were 92× 10^6, 43× 10^5 and 38 × 10^5, respectively, on day 3. The bacterial count in these wounds was greater than 1× 10^5 which considered to be infected.[35] The mean count of the bacteria per gram of tissue in PC group was 42× 10^4. There were not any significant differences in bacterial count within the treatment groups on days 7 and 14 post-wounding (P > 0.05). The count of bacteria in these wounds was lower than 1× 10^5. A minimum bacterial count was achieved at PC group in the study period (P < 0.05).

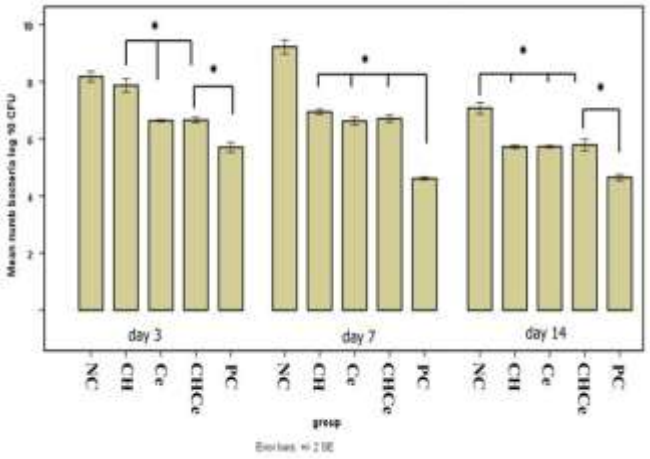

Figure 11. The mean number of bacteria $\log_{10}$ CFU/wound in different groups.

Discussion

The healing effect of chitosan supported nano-CeO2 on rat experimental excisional wound infected with *p. aeruginosa* was investigated in the present study. The therapeutic properties of chitosan supported CeO2 on the infected wound was comparable to 1% silver sulfadiazine ointment which was effectively used to control *P. aeruginosa* in wounds.[6,7]

In the present study the higher rate of wound closure was achieved in the treatment groups especially in topical application of chitosan supported nano-CeO2 compared to NC group. The role of nano-CeO2 to enhance proliferation and migration of keratinocytes in the processes of wound healing is noticeable.[17] The shape, size and physiochemical properties of nanoparticles are very important for its biological applications and in a recent study, topical application of chitosan caused significant reduction in wound size.[18] In the present study we engineered CeO2 nanoparticles in appropriate size of 4.9-6.2 nm that embedded on chitosan gel to improve its physiochemical properties.[20,36]

The lower PMNL cells infiltration in the treatment groups compared to NC group in our study could be resulted from the positive effects of the wound infection controlled by chitosan supported nanocerium due to rapid infiltration of PMNL cells into wound area, scale 2 for ChCe group on day 3. It has also been reported that local application of chitosan could enhance the functions of PMNL cells.[34]

The higher fibroblast proliferation on days 3 and 7 in the treatment groups compared to NC group in this study could be resulted from 1) the strong stimulation effect of chitosan on fibroblast to proliferate in the wound bed and 2) the positive effects of nanocerium in enhancing fibroblast migration and proliferation.[17,35,36]

The higher collagen deposition in the treatment groups compared to NC group in this study could be resulted from the positive effect of nanocerium and chitosan in producing high amount of collagen.[34,37] The amount of hydroxyproline level has been reported be increased with topical application of nanocerium in incisional wound.[37]

In the present study, higher levels of hydroxyproline in the treatment groups compared to NC group were in accordance with the amount of collagen deposition in the wound. In this study the higher neovascularization scale in the treatment groups compared to NC group was seen on days 3 and 7. The positive effect of nanocerium in promotion of angiogenesis has been reported and it has been reported that chitosan hydrogel has an ability to induce neovascularization in wound healing.[38] Higher neovascularization represents an important process in defending the wound against infection because of supplying the wound with oxygen, immunoglobulins and white blood cells which are necessary to cope with infection.[24]

FRAP approved to be quick and simple comparable method for antioxidant capacity scanning in tissues.[39] Higher total antioxidant capacity in treatment groups compared to NC group in this study might be related to the antioxidant effects of chitosan and nanocerium in the wound healing.[40] The ability of nanocerium in enhancing wound healing may be due to its dual oxidation states and promoting free radical scavenging activity at the site of wound.[37] The total antioxidant capacity was higher in ChCe group compared to those of CH and Ce groups on day 14. This positive effect may cause a synergistic effect among chitosan gel and nanocerium particles. Chitosan not only can enlarge the stability of nanocerium but can retain its excellent antioxidative activity.[41] It seems the antioxidant capacity of chitosan supported-nanocerium could be preserved for several (at least 7, days in local application on excisional wound. Topical application of antioxidants in addition to their direct effect on free radicals can also protect collagen and glycosaminoglycans from oxidation, which may help enhance infected wound healing.[42]

On day 3, the mean bacterial count in the treatment groups showed local application of chitosan, nanocerium and chitosan supported-nanocerium were unable to convert the experimental infected wound into contaminated wound despite large reduction in the bacterial count. However, continuing these treatments until day 7 was able to convert the infected wound into contaminated wound and the antibacterial effect of the treatments lasted until day 14 post-wounding.

Overall, in the present study the results of histopathological findings were consistent with those of TAC and bacteriological assessments. A significant enhanced tissue formation and re-epithelialization, lower PMNL cells infiltration, higher collagen deposition, higher levels of hydroxyproline content, higher neovascularization scale, enhancement of total antioxidant capacity and reduction of the bacterial load treated with chitosan supported nano-CeO2 could be comparable to the use of 1% silver sulphadiazine ointment in positive control group suggesting a therapeutic potential in the infected excisional wound healing. Chitosan supported nano-CeO2 could be suggested as an alternative

antimicrobial agent in the treatment of infected wounds. Chitosan supported nano-CeO2 could help prevent development of antimicrobial resistance. CNPs are well tolerated in both *in vitro* and *in vivo* in biological models. [43]

It was concluded that topical application of chitosan supported nano-CeO2 could accelerate the healing process of experimental infected excisional dermal wound in a rat model. In particular, engineered chitosan supported nano-CeO2 could enhance tissue total antioxidant capacity, reduce the bacterial count, accelerate proliferation and migration of fibroblasts and keratinocytes, increase hydroxyproline level and neovascularization scale of the healing wound. This study suggested the potential therapeutic effects of the engineered chitosan supported nano-CeO2 for topical treatment on infected wounds with *p. aeruginosa*.

Acknowledgment

This work was financially supported by the Faculty of Veterinary Medicine of Urmia University, Urmia, Iran. The results described in this paper were part of student thesis.

Conflicts of interest

None

Reference

1. Bitar MS, Al-Mulla F. ROS constitute a convergence nexus in the development of IGF1 resistance and impaired wound healing in a rat model of type 2 diabetes. *Disease Models and Mechanisms*, 2012; 5(3): 375-388.
2. Robson MC. Wound infection: a failure of wound healing caused by an imbalance of bacteria. *Surgical Clinics of North America*, 1997;77(3):637-650.
3. Barrientos S, Stojadinovic O, Golinko M. Brem H, Tomic-Canic M. Growth factors and cytokines in wound healing. *Wound Repair and Regeneration*, 2008;16(5): 585-601.
4. Societies WU, Wound infection in clinical practice. An international consensus. *International of Wound Journal*, 2008; 5(Suppl 3): 1-11.
5. Murray PR, Rosenthal KS, Pfaller MA, Medical microbiology. pseudomonas and related bacteria 2015, Elsevier Health Sciences. 7th Edition: 2013 by Saunders, an imprint of Elsevier Inc. chapter 30 .p. 291-293
6. Fox CL. Silver sulfadiazine- a new topical therapy for pseudomonas in burns: therapy of pseudomonas infection in burns. *Archives of Surgery*, 1968;96(2): 184-188.
7. Hollinger MA. Toxicological aspects of topical silver pharmaceuticals. *Critical Reviews in Toxicology*, 1996;26(3):255-260.
8. Schäfer M, Werner S. Oxidative stress in normal and impaired wound repair. *Pharmacological Research*, 2008;58(2): 165-171.
9. Rasik AM, Shukla A. Antioxidant status in delayed healing type of wounds. *International journal of experimental pathology*, 2000;81(4): 257-263.
10. Pehr K, Forsey RR. Why don't we use vitamin E in dermatology? *Canadian Medical Association Journal*, 1993; 149(9):1247.
11. Sidhu GS, Singh AK, Thaloor D, Banaudha KK, Patnaik GK, Srimal RC, Maheshwari RK. Enhancement of wound healing by curcumin in animals. *Wound Repair and Regeneration*, 1998;6(2):167-177.
12. Narayanan S, Sathy BN, Mony U, Koyakutty M, Nair SV, Menon D. Biocompatible magnetite/gold nanohybrid contrast agents via green chemistry for MRI and CT bioimaging. *ACS applied materials & interfaces*, 2011;4(1):251-260.
13. Darroudi M, Sabouri Z, Oskuee RK, Zak AK, Kargar H, Hamid MHNA. Green chemistry approach for the synthesis of ZnO nanopowders and their cytotoxic effects. *Ceramics International*, 2014; 40(3):4827-4831.
14. Darroudi M, Sabouri Z, Oskuee RK, Zak AK, Kargar H. Hamid MHNA. Sol–gel synthesis, characterization, and neurotoxicity effect of zinc oxide nanoparticles using gum tragacanth.

Ceramics International, 2013;39(8): 9195-9199.
15. Hamdan S, Pastar I, Drakulich S, Dikici E, Tomic-Canic M, Deo S, Daunert S. Nanotechnology-Driven Therapeutic Interventions in Wound Healing: Potential Uses and Applications. *ACS Central Science*, 2017; 3(3):163.
16. Wason MS, Zhao J. Cerium oxide nanoparticles: potential applications for cancer and other diseases. *American Journal of Translational Research,* 2013; 5(2):126-131.
17. Chigurupati S, Mughal MR, Okun E, Das S, Kumar A, McCaffery M, Mattson MP. Effects of cerium oxide nanoparticles on the growth of keratinocytes, fibroblasts and vascular endothelial cells in cutaneous wound healing. *Biomaterials,* 2013; 34(9): 2194-2201.
18. Alsarra IA, Chitosan topical gel formulation in the management of burn wounds. *International journal of biological macromolecules,* 2009;45(1): 16-21.
19. Azuma K, Izumi R, Osaki T, Ifuku S, Morimoto M, Saimoto H, Okamoto Y. Chitin, chitosan, and its derivatives for wound healing: Old and new materials. *Journal of functional biomaterials*, 2015; 6(1):104-142.
20. Anjum S, Arora A, Alam MS, Gupta B. Development of antimicrobial and scar preventive chitosan hydrogel wound dressings. *International journal of pharmaceutics,* 2016;508(1):92-101.
21. Sudarshan N, Hoover D, Knorr D, Antibacterial action of chitosan. *Food Biotechnology*, 1992;6(3):257-272.
22. Chung Y-C, Chen C-Y. Antibacterial characteristics and activity of acid-soluble chitosan. *Bioresource Technology*, 2008; 99(8):2806-2814.
23. dos Santos CCL, Farias IAP, dos Reis Albuquerque ADJ, de Silva PMDF, da Costa One GM, Sampaio FC. Antimicrobial activity of nano cerium oxide (IV)(CeO2) against Streptococcus mutans. BMC Proc. 2014;8(Suppl 4):48.
24. Nascimento EGd, Sampaio TBM, Medeiros AC, Azevedo EPD. Evaluation of chitosan gel with 1% silver sulfadiazine as an alternative for burn wound treatment in rats. *Acta Cirurgica Brasileira,* 2009; 24(6):460-465.
25. Negahdary M, Mohseni G, Fazilati M, Parsania S, Rahimi G, Rad S. RezaeiZarchi S. The Antibacterial effect of cerium oxide nanoparticles on Staphylococcus aureus bacteria. *Annals of Biological Research* 2012;3(7):3671-3678.
26. Kuang Y, He X, Zhang Z, Li Y, Zhang H, Ma Y, Chai Z. Comparison study on the antibacterial activity of nano-or bulk-cerium oxide. *Journal of nanoscience and nanotechnology*, 2011; 11(5): 4103-4108.
27. Zimmermann M. Ethical guidelines for investigations of experimental pain in conscious animals. *Pain*, 1983;16(2): 109-110.
28. Gautam MK, Purohit V, Agarwal ., Singh, A, Goel RK. In vivo healing potential of Aegle marmelos in excision, incision, and dead space wound models. *The Scientific World Journal*, 2014 Article ID 740107, 9 pages.
29. Gal P, Kilik R, Mokry M, Vidinsky B, Vasilenko T, Mozes S, Lenhardt L. Simple method of open skin wound healing model in corticosteroid-treated and diabetic rats: standardization of semi-quantitative and quantitative histological assessments. *Veterinary Medecine,* 2008; 53(12): 652-659.
30. Greenhalgh DG, Sprugel KH, Murray MJ, Ross R. PDGF and FGF stimulate wound healing in the genetically diabetic mouse. *The American journal of pathology*, 1990; 136(6):1235.
31. Dos Santos ML, Lima RC, Riccardi CS, Tranquilin RL, Bueno PR, Varela JA, Longo E. Preparation and characterization of ceria nanospheres by microwave-hydrothermal method. *Materials Letters,* 62(30),4509-4511.
32. Benzie IF, Strain J. Ferric reducing/antioxidant power assay: Direct measure of total antioxidant activity of biological fluids and modified version for simultaneous measurement of total

antioxidant power and ascorbic acid concentration. *Methods in enzymology,* 1999; 299:15-27.

33. Harley J, Prescott L. Bacterial Morphology and Staining. Laboratory Exercises in Microbiology, 5th Edition, The McGraw-Hill Companies, New York, 2002;31-36.
34. Ueno H, Mori T, Fujinaga T. Topical formulations and wound healing applications of chitosan. *Advanced drug delivery reviews,* 2001;52(2):105-115.
35. Howling GI, Dettmar PW, Goddard PA, Hampson FC, Dornish M,Wood EJ. The effect of chitin and chitosan on the proliferation of human skin fibroblasts and keratinocytes in vitro. *Biomaterials,* 2001; 22(22): 2959-2966.
36. Chen S-H, Tsao CT, Chang CH, Lai YT, Wu MF, Chuang CN, Hsieh KH. Assessment of reinforced poly (ethylene glycol) chitosan hydrogels as dressings in a mouse skin wound defect model. *Materials Science and Engineering: C,* 2013;33(5):2584-2594.
37. Davan R, Prasad RGSV, Jakka VS, Aparna RSL, Phani AR, Jacob B, Raju DB. Cerium oxide nanoparticles promotes wound healing activity in in-vivo animal model. *Journal of Bionanoscience,* 2012; 6(2):78-83.
38. Ishihara M, Obara K, Ishizuka T, Fujita M, Sato M, Masuoka K, Kikuchi M. Controlled release of fibroblast growth factors and heparin from photocrosslinked chitosan hydrogels and subsequent effect on in vivo vascularization. *Journal of Biomedical Materials Research Part A,* 2003;64(3):551-559.
39. Katalinic V, Modun D, Music I, Boban M. Gender differences in antioxidant capacity of rat tissues determined by 2, 2′-azinobis (3-ethylbenzothiazoline 6-sulfonate; ABTS) and ferric reducing antioxidant power (FRAP) assays. *Comparative Biochemistry and Physiology Part C: Toxicology & Pharmacology,* 2005; 140(1): 47-52.
40. Korsvik C, Patil S, Seal S, Self WT. Superoxide dismutase mimetic properties exhibited by vacancy engineered ceria nanoparticles. *Chemical communications,* 2007;10:1056-1058.
41. Zhai Y, Zhou K, Xue Y, Qin F, Yang L, & Yao X. Synthesis of water-soluble chitosan-coated nanoceria with excellent antioxidant properties. *Rsc Advances,* 2013;3(19):6833-6838.
42. Sen CK, Khanna S, Gordillo G, Bagchi D, Bagchi M, Roy S. Oxygen, oxidants, and antioxidants in wound healing. *Annals of the New York Academy of Sciences,* 2002. 957(1):239-249.
43. Das S, Dowding JM, Klump KE, McGinnis JF, Self W, Seal S. Cerium oxide nanoparticles: applications and prospects in nanomedicine. *Nanomedicine,* 2013; 8(9): 1483-1508.

نشریه جراحی دامپزشکی ایران
سال۲۰۱۷ ، جلد ۱۲ (شماره ۲)، شماره پیاپی ۲۷

چکیده

اثر ترمیمی کیتوزان –نانوسریم بر روی زخم تمام ضخامت تجربی عفونی شده با سودوموناس آئروژنیزا در رت

آکو شبرندی[۱]، سعید عزیزی[۱]، رحیم حب نقی[۲]، عبدالغفار اونق[۳]، سجاد کشی پور[۴]

[۱]گروه جراحی و تصویربرداری تشخیصی، دانشکده دامپزشکی، دانشگاه ارومیه، ارومیه، ایران.

[۲]گروه پاتوبیولوژی، دانشکده دامپزشکی، دانشگاه ارومیه، ارومیه، ایران.

[۳]گروه میکروبیولوژی، دانشکده دامپزشکی، دانشگاه ارومیه، ارومیه، ایران.

[۴]گروه نانوشیمی، مرکز تحقیقات نانوتکنولوژی، دانشگاه ارومیه، ارومیه، ایران.

هدف- اثر ترمیمی کیتوزان حمایت شده با نانوذره سریم اکسید بر روی زخم تمام ضخامت تجربی عفونی شده با سودوموناس آئروژنیزا در مدل حیوانی موش صحرایی مورد مطالعه قرار گرفت.

طرح- مطالعه تجربی

حیوانات- ۶۰ سر موش صحرایی نر نژاد آلبینو

روش کار- ابتدا هیدروژل کیتوزان حمایت شده با نانوذره سریم اکسید تهیه شد. خصوصیت آن با انجام آزمایشات FT-IR، EDX ، XRD ، SEM و TEM تایید گردید. ابتدا زخم با باکتری سودوموناس آئروژنیزا عفونی شده و در گروه کنترل مثبت با پماد سولفادیازین- نقره درمان شده و در گروه کنترل منفی هیچگونه درمانی بر روی زخم صورت نگرفت. زخم عفونی با ژل کیتوزان، محلول نانوذره سریم اکسید و ژل کیتوزان-نانوسریم به ترتیب در گروه های کیتوزان، سریم و کیتوزان-سریم درمان شد. موش های صحرایی به طور تصادفی در ۵ گروه ۱۲ سری تقسیم شدند. هرگروه دوباره به سه زیرگروه شامل ۴ سر موش صحرایی تقسیم شده و در روزهای ۳، ۷ و ۱۴ روند بهبودی زخم مورد مطالعه قرار گرفت.

نتایج - ارزیابی های پلانی متری، هیستوپاتولوژی و میزان هیدروکسی پرولین نشان داد که ترمیم زخم عفونی تمام ضخامت پوستی در گروه های درمانی به خصوص در گروه کیتوزان-سریم در مقایسه با گروه کنترل منفی بهتر و زودتر به انجام می رسد ($P < 0.05$). با انجام آزمایش FRAP ، ظرفیت آنتی اکسیدانتی تام در گروه های درمانی در مقابسه با گروه کنترل منفی به طور معنی داری بیشتر بود ($P < 0.05$). تعداد باکتری در گروه کیتوزان-سریم و گروه سریم در مقایسه با گروه کیتوزان به طور معنی داری در روز ۳ کمتر بود ($P < 0.05$).

نتیجه گیری و کاربرد بالینی- کاربرد موضعی ژل بر روی زخم عفونی موجب افزایش ظرفیت آنتی اکسیدانتی تام، کاهش تعداد باکتری، تسریع پرولیفراسیون و مهاجرت فیبروبلاست ها و کراتینوسیت ها، افزایش میزان هیدروکسی پرولین و شاخص نو رگ زایی در ترمیم زخم می شود. هیدروژل کیتوزان - نانو سریم اکسید می تواند به عنوان یک جانشین برای درمان زخم های عفونی به کار رود.

واژ گان کلیدی : نانوذره سریم اکسید – کیتوزان، نانوذره سریم اکسید، کیتوزان، سودوموناس آئروژنیزا، ترمیم زخم، موش صحرایی